

# BOUNDARY CONDITIONS IN SHALLOW WATER MODELS— AN ALTERNATIVE IMPLEMENTATION FOR FINITE ELEMENT CODES

R. L. KOLAR\*

*School of Civil Engineering and Environmental Science, University of Oklahoma, Norman, OK 73019, U.S.A.*

AND

W. G. GRAY AND J. J. WESTERINK

*Department of Civil Engineering and Geological Sciences, University of Notre Dame, Notre Dame, IN 46556, U.S.A.*

## SUMMARY

Finite element solution of the shallow water wave equations has found increasing use by researchers and practitioners in the modelling of oceans and coastal areas. Wave equation models, most of which use equal-order  $C^0$  interpolants for both the velocity and the surface elevation, do not introduce spurious oscillation modes, hence avoiding the need for artificial or numerical damping. An important question for both primitive equation and wave equation models is the interpretation of boundary conditions. Analysis of the characteristics of the governing equations shows that for most geophysical flows a single condition at each boundary is sufficient, yet there is not a consensus in the literature as to what that boundary condition must be or how it should be implemented in a finite element code. Traditionally (partly because of limited data), surface elevation is specified at open ocean boundaries while the normal flux is specified as zero at land boundaries. In most finite element wave equation models both of these boundary conditions are implemented as essential conditions. Our recent work focuses on alternative ways to numerically implement normal flow boundary conditions with an eye towards improving the mass-conserving properties of wave equation models. A unique finite element formulation using generalized functions demonstrates that boundary conditions should be implemented by treating normal fluxes as natural conditions with the flux interpreted as external to the computational domain. Results from extensive numerical experiments show that the scheme does conserve mass for all parameter values. Furthermore, convergence studies demonstrate that the algorithm is consistent, as residual errors at the boundary diminish as the grid is refined.

KEY WORDS: shallow water equations; wave continuity equation; boundary conditions; finite elements; generalized functions

## BACKGROUND

Shallow water equations are obtained by vertically averaging the time-averaged microscopic mass and momentum balances over the depth of the water column. Early finite element solutions of the shallow water equations were often plagued by spurious oscillations.<sup>1</sup> Various methods were introduced to eliminate the oscillations, but all included some type of artificial damping. Lynch and Gray<sup>2</sup> and Gray<sup>3</sup> present the wave continuity equation as a means to avoid spurious oscillations without resorting to numerical or artificial damping of the solution. Since the inception of the wave continuity formulation in 1979, the original algorithm has been modified in a number of substantial ways: a numerical

\* Formerly at Department of Civil and Environmental Engineering, University of New Haven, West Haven, CT 06516, U.S.A.

parameter was introduced to provide a more general means of weighting the primitive continuity equation,<sup>4</sup> viscous dissipation terms were incorporated<sup>5,6</sup> and three-dimensional simulations were realized by resolving the velocity or stress profile in the vertical.<sup>7-10</sup> The resulting algorithm has been extensively tested using analytical solutions and field data and is currently being used by researchers and practitioners to model the hydrodynamic behaviour of coastal and oceanic regions.<sup>11-15</sup>

In the course of some of the applications it was discovered that when non-linear components of the solution are significant, the wave continuity equation in its original form does not conserve mass. Two methods of mitigating the errors are presented in Reference 16. In the first it is shown that if  $G$ , the numerical parameter in the generalized wave continuity equation, is increased so that its value is one or two orders of magnitude larger than the bottom friction, then mass conservation is greatly improved. However, an upper bound on  $G$  exists, above which the solution becomes too primitive and spurious oscillations appear in the solution. Dispersion analysis can be used as a tool to *a priori* predict the maximum value of  $G$ . In lieu of dispersion analysis, experimental results suggest using a value of  $G/\tau_{\max}$  on the order of 1–10, where  $\tau$  is the non-linear bottom friction. The second mitigation technique reformulates the convective term in the generalized wave continuity equation so that a consistency exists between the momentum and continuity equations (e.g. both equations cast the advective terms in non-conservative form). If both mitigating measures are used in conjunction, then global mass balance errors are eliminated while errors in local regions (even individual elements) are virtually non-existent except for regions near the open boundaries. One- and two-dimensional applications demonstrate the effectiveness of the procedure. However, the persistence of mass balance errors near open boundaries led to this study of the influence of boundary conditions on mass conservation and solution accuracy.

The outline of the article is as follows. After presenting the governing equations and discretization technique, the history of boundary conditions, as implemented in finite element shallow water models, is examined. An alternative interpretation of flux terms that appear in boundary integrals is proposed; the interpretation is justified by deriving the finite element equations using generalized functions (multidimensional Heaviside step functions and Dirac delta functions). With this unique approach, boundary conditions fall out naturally during the derivation rather than being implemented in an *ad hoc* fashion as is done with many conventional formulations.<sup>4,7,17-19</sup> Numerical experiments and convergence studies demonstrate the effectiveness of the algorithm.

## CONSERVATION EQUATIONS

Primitive forms of the balance laws are obtained by vertical averaging of the time-averaged microscopic balance laws. With operator notation the primitive form of the continuity equation is presented as

$$L \equiv \frac{\partial \zeta}{\partial t} + \nabla \cdot (H\mathbf{v}) = 0. \quad (1)$$

The conservative form of conservation of momentum is given by

$$\mathbf{M}^c \equiv \frac{\partial (H\mathbf{v})}{\partial t} + \nabla \cdot (H\mathbf{v}\mathbf{v}) + \tau H\mathbf{v} + H\mathbf{f} \times \mathbf{v} + gH\nabla\zeta - \mathbf{A} - \frac{1}{\rho} \nabla \cdot (H\mathbf{T}) = 0 \quad (2)$$

and the non-conservative form of conservation of momentum is given by

$$\mathbf{M} \equiv \frac{1}{H} (\mathbf{M}^c - \mathbf{v}L) = 0. \quad (3a)$$

Substituting (1) and (2) into (3a) gives

$$\mathbf{M} \equiv \frac{\partial \mathbf{v}}{\partial t} + \mathbf{v} \cdot \nabla \mathbf{v} + \tau \mathbf{v} + \mathbf{f} \times \mathbf{v} + g \nabla \zeta - \frac{\mathbf{A}}{H} - \frac{1}{\rho H} \nabla \cdot (H\mathbf{T}) = 0. \quad (3b)$$

In operator form the generalized wave continuity (GWC) equation is

$$W^G \equiv \frac{\partial L}{\partial t} + GL - \nabla \cdot \mathbf{M}^c = 0. \quad (4a)$$

Substituting (1) and (2) into (4a) gives

$$W^G \equiv \frac{\partial^2 \zeta}{\partial t^2} + G \frac{\partial \zeta}{\partial t} + (G - \tau) \nabla \cdot (H\mathbf{v}) - \nabla \cdot \left( \nabla \cdot (H\mathbf{v}\mathbf{v}) + H\mathbf{f} \times \mathbf{v} + gH\nabla \zeta - \mathbf{A} - \frac{1}{\rho} \nabla \cdot (H\mathbf{T}) \right) - H\mathbf{v} \cdot \nabla \tau = 0. \quad (4b)$$

The wave continuity equation, as it originally appeared in Reference 2, is obtained by setting  $G = \tau$ . Also note that the primitive continuity equation can be viewed as a limiting form of the generalized wave continuity equation by letting  $G \rightarrow \infty$ .

## DISCRETIZATION

Equations (1), (2), (3b) and (4b) are discretized in space using a standard Galerkin finite element approximation with linear elements. Implicit time discretization of  $L$  and  $W^G$  uses a three-time-level approximation centred at  $k$ . Time discretization for  $\mathbf{M}$  and  $\mathbf{M}^c$  uses a lumped two-time-level approximation centred at  $k + \frac{1}{2}$ ; the advective terms are formulated explicitly, resulting in a system of linear algebraic equations. Exact quadrature rules are employed. The resulting discretized equations can be found in Reference 7. A sequential solution procedure is adopted where the continuity equation ((1) or (4b)) is used to solve for elevations and the momentum equation ((2) or (3b)) is used to solve for the velocity field.

## BOUNDARY CONDITIONS

The governing conservation equations represent a coupled hyperbolic system of partial differential equations that describe the propagation of long water waves in shallow water. As such, characteristic theory is an appropriate tool to study proper specification of boundary conditions. In particular, for the primitive conservation equations it has been shown that one condition on each physical boundary is required (in addition to initial conditions for the 'time boundary'). Drolet and Gray<sup>20</sup> extended the analysis of characteristic planes to the wave continuity equation and determined that a single boundary condition is still sufficient for conditions normally encountered in geophysical simulations.

Mathematically the conditions are specified as one of three types: Dirichlet (type I) in which the value of the dependent variable is specified, Neumann (type II) in which the value of the flux is specified and Robin (type III) which is a linear combination of the first two. In shallow water modelling, these types describe the physical situations of known elevation, known flux and stage discharge relations respectively (the latter is often referred to as a radiation boundary condition). This article focuses on the first two types of conditions. In finite element vernacular a Dirichlet condition means that the value of the dependent variable is known on the boundary; it is referred to as an essential condition. A specified flux condition enters the right-hand-side vector in the discrete set of equations and is referred to as a natural boundary condition.

For a single partial differential equation with one dependent variable, such as Laplace's equation or the diffusion equation, specified boundary conditions fall neatly into one of the above categories and implementation is unambiguous. Unfortunately, such is not the case for the coupled hyperbolic system at hand, for what may serve as an essential condition for the momentum equation may equally be interpreted as a natural condition for the continuity equation. This ambiguity has led to an inconsistent treatment of boundary conditions in the literature;<sup>1,4,7,17-19,21-23</sup> to date, there appears to be no consensus on the 'best' way to implement the conditions. Complicating the matter is the fact that data often dictate what information is available at the boundary. For example, elevation data, either from global tidal models or from field measurements, are more reliable and more prevalent than are velocity data. The end result is that the researcher is often faced with the task of choosing one interpretation over the other, which frequently is tantamount to choosing which boundary equation to discard.

Lynch<sup>24</sup> was one of the first to study the affect of boundary conditions on mass conservation in the context of the wave continuity algorithm. Using well-known properties of linear basis functions, i.e. the sum of the functions over all elements is equal to one and the sum of the gradient of the basis functions over all elements is zero, he demonstrates that all terms of the continuity equation must be retained in order to maintain global conservation of mass, regardless of the nature of the boundary data. He refers to this interpretation of the boundary conditions as mass conservative boundary conditions. However, several open issues remain. For example, it is not clear how momentum conservation is affected by this interpretation, an equally important consideration.

Guided by the work of Lynch<sup>24</sup> and others,<sup>25-29</sup> we hypothesize that when Green's theorem is applied to the flux term during finite element formulation of the continuity equation, the flux in the boundary integral should be interpreted as *external* to the computational domain. Thus it becomes an additional unknown in the discrete set of equations. In addition to guaranteeing global mass balance, this formulation balances the number of equations plus boundary conditions with the number of unknowns; hence neither data nor boundary equations are discarded.

#### DERIVATION

For clarity, consider just the flux term  $\nabla \cdot \mathbf{Q}$ , where  $\mathbf{Q} = H\mathbf{v}$ , in equation (1) or (4b) during the finite element formulation. In a conventional finite element formulation one discretizes the domain of interest  $\Omega$  using appropriate elements and applies Green's theorem to the flux term to yield

$$\int_{\Omega} \nabla \cdot \mathbf{Q} \varphi_i \, d\Omega = - \int_{\Omega} \mathbf{Q} \cdot \nabla \varphi_i \, d\Omega + \int_{\partial\Omega} \mathbf{n} \cdot \mathbf{Q} \varphi_i \, d\Gamma, \quad (5)$$

where  $\partial\Omega$  is the boundary of the discretized domain. In (5) it is not clear how to interpret the flux  $\mathbf{Q}$  that appears in the boundary integral, especially if one uses equal-order  $C^0$  interpolants, i.e. is  $\mathbf{Q}$  internal or external to the domain? Also, if it is internal, how does this value relate to the momentum equation?

Boundaries, and hence boundary conditions, arise from the artificial restriction of a global problem to a localized study region; the boundary conditions link the characteristics of the local problem to the outside world. Our philosophy is that to properly interpret and implement boundary conditions, the boundaries should be kept internal to the domain during the finite element formulation so that the proper link to the outside world is maintained. This approach is realized by first discretizing the *entire* global region and then using generalized functions to delineate local study regions with their corresponding boundaries. It is during the problem formulation that the boundary conditions develop naturally in a clear and unambiguous manner. The methodology was first presented by Gray and Celia<sup>30</sup> for an elliptic problem; here we adapt the procedure to hyperbolic problems.

Consider again just the flux term from the continuity equation (minus any coefficients) so that the equation to be discretized is given by

$$\nabla \cdot \mathbf{Q} = 0. \quad (6)$$

The first step is to discretize all space  $\Omega_\infty$  into  $N$  triangular elements (the element shape is arbitrary). Discretizing all space with a finite number of elements presents no conceptual problem if one visualizes all space as the spherical earth rather than an infinite plane. Next approximate  $\mathbf{Q}$  with (summation implied)

$$\mathbf{Q} \approx \mathbf{Q}_e \gamma_e, \quad (7)$$

where  $\mathbf{Q}_e$  is a piecewise polynomial approximation of  $\mathbf{Q}$  inside the domain of interest ( $\Omega$ ),  $\gamma_e$  is a generalized Heaviside step function that has a value of one in element  $e$  and zero outside, and the summation is over all elements in  $\Omega_\infty$ . It is important to recognize that  $\gamma_e$  in (7) is *not* an interpolating polynomial and  $\mathbf{Q}_e$  is *not* a nodal coefficient. Outside of  $\Omega$  the choice of approximating functions is arbitrary; a reasonable choice is to select  $\mathbf{Q}_e$  so that it satisfies the governing differential equation exactly.

A finite element approximation can be obtained by weighting (6) with a set of polynomial weighting functions,  $\varphi_i$  and integrating the result over all space. The only requirement we impose on  $\varphi_i$  is that it have a value of one at node  $i$  and zero at all other nodes. Equation (6) then becomes (summation implied)

$$\int_{\Omega_\infty} \nabla \cdot (\mathbf{Q}_e \gamma_e) \varphi_i \, d\Omega = 0 \quad \text{for } i = 1, \dots, N. \quad (8)$$

Next expand the spatial derivative in (8) to obtain (summation implied)

$$\int_{\Omega_\infty} \gamma_e \nabla \cdot \mathbf{Q}_e \varphi_i \, d\Omega + \int_{\Omega_\infty} \mathbf{Q}_e \cdot \nabla \gamma_e \varphi_i \, d\Omega = 0 \quad \text{for } i = 1, \dots, N. \quad (9)$$

Since  $\gamma_e = 1$  inside an element, the value of the first integral is not affected by  $\gamma_e$ , so it will be dropped from this integrand in ensuing equations.

In Reference 31 it is shown that the gradient of the generalized Heaviside step function is a multidimensional Dirac function, namely

$$\nabla \gamma_e = -\mathbf{n}_e \delta(\mathbf{x} - \mathbf{x}_e),$$

where  $\mathbf{x}_e$  is the locus of point forming the boundary of element  $e$  and  $\mathbf{n}_e$  is a unit outward normal from element  $e$ . Integral properties of (10) are analogous to the familiar one-dimensional Dirac function,<sup>31</sup> i.e.

$$\int_{\Omega_\infty} \mathbf{f} \cdot \nabla \gamma_e \, d\Omega = - \int_{\partial\Omega_e} \mathbf{n}_e \cdot \mathbf{f} \, d\Gamma. \quad (11)$$

Now, to interpret equation (9), consider two separate regions of the global domain  $\Omega$ : (i)  $i$  is a node inside  $\Omega$ ; (ii)  $i$  is a node on the boundary of  $\Omega$ . Recall that outside of  $\Omega$ ,  $\mathbf{Q}$  has been chosen to satisfy the governing equation, so no solution is required.

*Region (i):  $i$  inside  $\Omega$*

Using (11), one can write (9) as

$$\sum_e \left( \int_{\Omega_e} \varphi_i \nabla \cdot \mathbf{Q}_e \, d\Omega - \int_{\partial\Omega_e} \mathbf{n}_e \cdot \mathbf{Q}_e \varphi_i \, d\Gamma \right) = 0, \quad (12)$$

where  $\Omega_e$  is an element in  $\Omega$  and the sum is over all elements in  $\Omega$ . If we require  $\varphi_i$  and  $\mathbf{Q}_e$  to be continuous within an element, then the divergence theorem can be applied to the second term to yield

$$\sum_e \left( \int_{\Omega_e} \varphi_i \nabla \cdot \mathbf{Q}_e \, d\Omega - \int_{\Omega_e} \nabla \cdot (\mathbf{Q}_e \varphi_i) \, d\Gamma \right) = 0 \tag{13}$$

and the chain rule can be used to express (13) as

$$\sum_e \left( - \int_{\Omega_e} \mathbf{Q}_e \cdot \nabla \varphi_i \, d\Omega \right) = 0. \tag{14}$$

Thus, on the interior of the computational domain, (9) reduces to the familiar finite element result.

*Region (ii): i on the boundary of  $\Omega$*

Consider the expanded view of the domain  $\Omega_\infty$  as shown in Figure 1 that contains a portion of the boundary  $\partial\Omega$  which divides the computational domain  $\Omega$  from the rest of  $\Omega_\infty$ . Define  $E$  to be all elements that have node  $i$  in common—the sum of the shaded regions in Figure 1. Use (11) and the fact that  $\varphi_i$  is zero outside the shaded region to write (9) as

$$\sum_E \left( \int_{\Omega_E} \nabla \cdot \mathbf{Q}_E \varphi_i \, d\Omega - \int_{\partial\Omega_E} \mathbf{n}_E \cdot \mathbf{Q}_E \varphi_i \, d\Gamma \right) = 0, \tag{15}$$

where  $\Omega_E$  is an element in the shaded region  $E$ .

Define  $A$  to be those elements of  $E$  in the region of interest  $\Omega$  and  $B$  to be those elements of  $E$  outside. In Figure 1,  $A$  is the lighter shaded region and  $B$  is the darker shaded region. Then (15) can be broken into the two sums

$$\sum_A \left( \int_{\Omega_A} \nabla \cdot \mathbf{Q}_A \varphi_i \, d\Omega - \int_{\partial\Omega_A} \mathbf{n}_A \cdot \mathbf{Q}_A \varphi_i \, d\Gamma \right) + \sum_B \left( \int_{\Omega_B} \nabla \cdot \mathbf{Q}_B \varphi_i \, d\Omega - \int_{\partial\Omega_B} \mathbf{n}_B \cdot \mathbf{Q}_B \varphi_i \, d\Gamma \right) = 0. \tag{16}$$

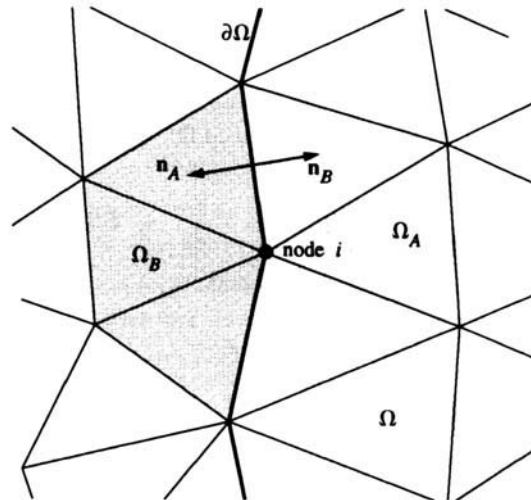


Figure 1. Expanded view of domain  $\Omega_\infty$  showing boundary  $\partial\Omega$  between the local region of interest (right of boundary) and remainder of domain (left of boundary). Region  $A$  is lighter and region  $B$  darker shaded region

Since  $B$  elements are external to the domain, the first integral in the  $B$  summation is zero (by our assumption that  $\mathbf{Q}_e$  exactly satisfies (6) outside of  $\Omega$ ). Apply the divergence theorem to the second integral in the  $A$  summation and then use the chain rule to combine it with the first integral to obtain

$$-\sum_A \left( \int_{\Omega_A} \mathbf{Q}_A \cdot \nabla \varphi_i \, d\Omega \right) - \sum_B \left( \int_{\partial\Omega_B} \mathbf{n}_B \cdot \mathbf{Q}_B \varphi_i \, d\Gamma \right) = 0. \quad (17)$$

Note that  $\mathbf{n}_B = -\mathbf{n}_A$ ; also, for the case considered here ( $i$  on the boundary of  $\Omega$ ),  $\varphi_i$  is non-zero only on the boundary between  $A$  and  $B$  elements, i.e. on the boundary of the computational domain,  $\partial\Omega$ . Thus (17) may be written as

$$-\sum_A \left( \int_{\Omega_A} \mathbf{Q}_A \cdot \nabla \varphi_i \, d\Omega \right) + \int_{\partial\Omega} \mathbf{n}_A \cdot \mathbf{Q}_B \varphi_i \, d\Gamma = 0. \quad (18)$$

In the second term,  $\mathbf{Q}_B$  is external to the domain, so its value can be chosen to produce the best solution in  $\Omega$ . An obvious choice is to select  $\mathbf{Q}_B$  such that  $\mathbf{n}_A \cdot \mathbf{Q}_B = 0$  on land boundaries and  $\mathbf{n}_A \cdot \mathbf{Q}_B$  is equal to the normal flux on open boundaries.

If one compares the result of the finite element formulation using generalized functions (equation (18)) with the results of a conventional formulation (equation (5)), it can be seen that the former leads to a result with a precise interpretation; namely, the boundary flux term that arises from application of Green's theorem is external to the computational domain.

In deriving this result, no continuity requirements between the polynomial approximation of  $\mathbf{Q}$  and the external flux value have been imposed. Thus there could conceivably be a discontinuity in flux at the boundary. Since flux in geophysical flows is continuous, such a discontinuity represents an error in the approximate (discrete) solution. However, errors are inherent in any numerical model. Conventional finite element formulations generally enforce continuity of flux at the boundaries by discarding an equation. The price one pays, in terms of approximating errors, for preserving flux continuity is mass balance errors. On the other hand, by treating boundary flux as external to the domain, no discrete equations are discarded and mass is conserved (demonstrated in the next section). Our opinion is that conserving mass locally and globally takes priority over flux continuity at the boundary, especially when coupling the hydrodynamic model to transport simulators. Furthermore, as will be shown in a following section, the flux at the boundary does become continuous as the grid is refined. Paralleling Gresho and Lee's theme of 'Don't suppress the wiggles—they're telling you something',<sup>32</sup> this residual error on the boundary can be used to indicate regions where the grid should be refined.

Finally, we note an additional feature of the proposed interpretation: boundary conditions in finite element codes are simpler to implement. Consider specifying a normal flux boundary condition in a conventional formulation. For  $C^0$  interpolants this flux is a nodal flux, and it is enforced as an essential condition. This requires that the momentum equation on the boundary be rotated to a normal-tangential co-ordinate system so that the specified condition can be enforced on only the normal component of velocity. Afterwards the solution must be rotated back to Cartesian (or spherical) co-ordinates. Keeping track of the orientation of unit normal vectors on irregular boundaries (those normally encountered in geophysical simulations) requires non-trivial coding. Furthermore, 'special edges', such as sharp corners on the boundary, require special processing of the data. In contrast, the proposed implementation, with normal flux values interpreted as external to the computational domain, obviates the need to rotate nodal momentum equations. Also, special edges require no special treatment.

## NUMERICAL VERIFICATION

The above formulation is tested in a series of one-dimensional experiments with results compared to a conventional formulation. A shallow one-dimensional east-west channel is used for the model problem so that significant non-linear components are generated, a situation that can give rise to mass balance errors.<sup>16</sup> Conditions for the problem are

channel co-ordinates	$0 \leq x \leq 50$ km
channel depth	5 m
eddy viscosity $\varepsilon$	$0.0 \text{ m}^2 \text{ s}^{-1}$
$\Delta t$	adjusted to maintain a Courant number $< 0.25$
$\Delta x$	2.5 km unless noted otherwise
$\lambda_{M_2}/\Delta x$	125 unless noted otherwise
boundary conditions	$\zeta(0, t) = 1.0 \sin(2\pi t/12.42 \text{ h}) \text{ m}$ $u(50, t) = 0.0 \text{ m s}^{-1}$
initial conditions	cold start: $\zeta(x, 0) = u(x, 0) = 0.0$
bottom friction $\tau$	$0.0001 \text{ s}^{-1}$ (constant).

The  $x$ -axis is defined positive to the east. The boundary conditions describe a channel with a land boundary at  $x = 50$  km being forced by an  $M_2$  tide with 1 m amplitude at  $x = 0$  km. Fine spatial resolution is used to minimize truncation error.

Mass conservation is checked globally and locally by comparing the time series of mass accumulation with cumulative net flux for the region of interest. Details of the algorithm are presented in Reference 16. Non-linear constituents are evaluated by decomposing the full solution into the  $M_2$  constituent, its steady state constituent and the  $M_4$  and  $M_6$  overtones using a least squares harmonic analysis.<sup>33,34</sup> Results are compared against a fine grid solution (320 elements,  $\Delta x = 0.156$  km,  $\lambda_{M_2}/\Delta x = 2000$ ).

Recall that conventional formulation of the boundary conditions treats all boundary information as essential conditions. Thus specified elevation results in a reduced matrix for the continuity equation and specified flux results in a reduced matrix for the momentum solution. This interpretation leads to gross mass balance errors; Figure 2 shows simulation results for the model problem using the conventional formulation. For perfect mass balance the two curves should overlay one another. (The

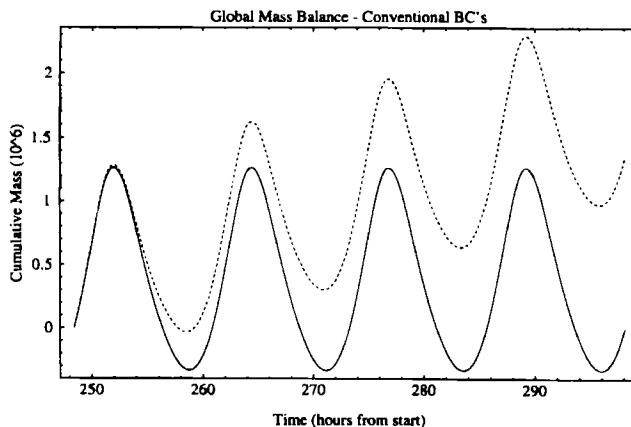


Figure 2. Global mass balance check of GWC formulation ( $G = \tau$ ; advective terms inconsistent) for model problem, conventional interpretation of boundary conditions. Full curve is accumulation; broken curve is net flux



mitigating procedures discussed earlier<sup>16</sup> are not implemented here so as to isolate the effect of boundary conditions; thus  $G/\tau$  is set to one and the advective terms are treated inconsistently.)

Under the proposed interpretation, state variables that appear in boundary integrals must be interpreted as external to the domain. For the one-dimensional finite element formulation of the primitive continuity equation (1), Green's theorem is applied to the flux term so that the weak form is given by

$$\left\langle \frac{\partial \zeta}{\partial t}, \varphi_i \right\rangle - \left\langle Hu, \frac{\partial \varphi_i}{\partial x} \right\rangle + Q|_{x_0^-}^{x_{N+}} = 0, \quad (19)$$

where nodes are numbered from 0 to  $N$ .

Under the proposed interpretation the boundary flux term  $Q = Hu$  is viewed as external to the domain, i.e. an unknown quantity. Hence the  $\pm$  designation in the limits of integration. In this way the number of equations plus boundary conditions is equal to the number of unknowns so that all information is used. No equations are discarded. Consequently, at the west boundary ( $i=0$ ) where  $\zeta$  is specified, elevation is known so that (19) is solved for external flux. That is, at  $i=0$  equation (19) becomes

$$Q_{0-} = \left\langle \frac{\partial \zeta}{\partial t}, \varphi_0 \right\rangle - \left\langle Hu, \frac{\partial \varphi_0}{\partial x} \right\rangle. \quad (20)$$

The momentum equation is then used to solve for velocity at the west boundary,  $u_{0+}$ . For comparison, consider implementation of this boundary condition in a conventional manner: the  $i=0$  equation is discarded from the set of discrete continuity equations, while the momentum equation is used to solve for the velocity at node 0.

At the east boundary ( $i=N$ ) the external flux is known so it enters the finite element formulation given in (19) naturally and the equation is solved for the unknown elevation. Thus at  $i=N$  equation (19) becomes

$$\left\langle \frac{\partial \zeta}{\partial t}, \varphi_N \right\rangle = \left\langle Hu, \frac{\partial \varphi_N}{\partial x} \right\rangle - Q_{N+}. \quad (21)$$

The momentum equation is then used to solve for the unknown velocity at the east boundary,  $u_{N-}$ . Recall that with this interpretation there may be a flux discontinuity at the boundary. For comparison, consider implementation of this boundary condition in a conventional manner: the specified flux enters an equation similar to (21) naturally, while the  $i=N$  equation is discarded from the set of discrete momentum equations.

When this external flux interpretation is applied to the GWC algorithm (the treatment of the flux term in the weak form of the GWC equation (4b) is analogous to its treatment in the primitive continuity equation as discussed above), simulation of the model problem results in no global mass balance error as shown in Figure 3 regardless of the value of the  $G$  parameter or the treatment of the advective terms.

To rigorously test the proposed algorithm, we set up the experimental matrix shown in Table I and computed three different error measures for each experiment: global mass balance error, local mass balance error and error in the generation of non-linear constituents. Results are summarized in Table II with ratings based on quantitative error measures. Also included in the table are results from experiments with a code using conventional treatment of the boundary conditions; these have been reported previously in Reference 16 but are included here for completeness.

As can be seen from the experimental results in Table II, the proposed algorithm conserves mass globally for all parameter values. However, local mass balance errors exist unless one formulates the advective terms consistently or uses a value of  $G$  two orders of magnitude larger than the bottom

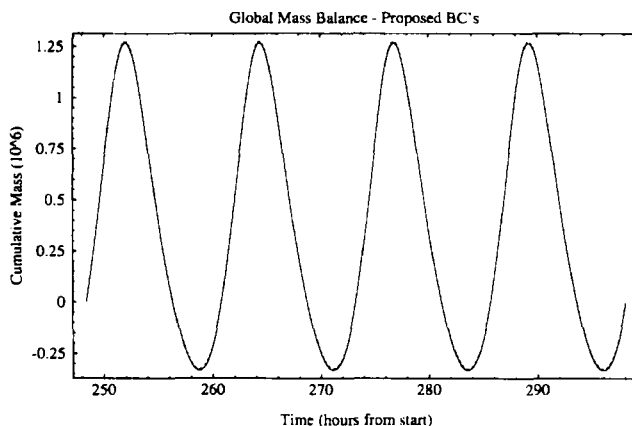


Figure 3. Global mass balance check of GWC formulation ( $G = \tau$ ; advective terms inconsistent) for model problem, proposed interpretation of boundary conditions. Full curve is accumulation; broken curve is net flux

friction  $\tau$ . Under either condition, local mass balance errors are minimal at the element level and they are virtually non-existent for local mass balance checks over two or more elements. In contrast, with conventional implementation of boundary conditions, local mass balance errors exist near the open ocean boundary for most parameter values. Constituent error between the two formulations behaves nearly identically; errors are large when  $G/\tau = 1$  and the advective terms are inconsistent; errors are reduced by treating the advective terms consistently; and for both of these situations the errors are virtually eliminated by increasing  $G/\tau$  to 100.

In summary, the results of the numerical experiments show that the proposed algorithm leads to less overall error than the corresponding conventional algorithm. Also, with the proposed algorithm, better results can be obtained for lower values of  $G$ , which is desirable for two-dimensional applications in order to avoid spurious oscillation modes. However, regardless of the value of  $G$  or the method used to implement boundary conditions, the advective terms should be formulated consistently in order to minimize mass balance error and to stabilize the simulator in highly non-linear applications.

In addition to the experiments shown in Table I, a large number of additional one-dimensional experiments were conducted, many of which looked at boundary conditions in mixed finite element formulations. Results parallel those presented herein; namely, solutions are more accurate and consistent using the proposed interpretation. This corroborates the findings of Sigurdsson<sup>27</sup> in his work with mixed finite element solution of the shallow water equations. One particularly interesting result is

Table I. Experimental matrix

Experiment number	Boundary conditions	Advective terms	$G/\tau$	Number of elements
1	Conventional	Not consistent	1.0	20
2	Conventional	Not consistent	100.0	20
3	Conventional	Consistent	1.0	20
4	Conventional	Consistent	100.0	20
5	Proposed	Not consistent	1.0	20
6	Proposed	Not consistent	100.0	20
7	Proposed	Consistent	1.0	20
8	Proposed	Consistent	100.0	20

Table II. Quantitative results of numerical experiments

Experiment number	Global mass balance	Local mass balance			Constituent error
		Ocean boundary	Interior	Land boundary	
1	*	*	***	****	*
2	***	***	****	*****	****
3	***	**	*****	****	***
4	****	****	****	****	****
5	*****	*	***	****	*
6	*****	****	****	****	****
7	*****	****	****	****	***
8	*****	****	****	****	****

Mass balance error (local and global) is computed as the mean of the absolute value of the difference between the time series of the net flux and the time series of accumulation over the last 4 days of the simulation.

Constituent error is computed as the mean of the absolute value of the difference between the amplitude of the steady state,  $M_2$ ,  $M_4$  and  $M_6$  components for each station and a fine grid solution (320 elements,  $\Delta x = 0.156$  km,  $\lambda_{M_i}/\Delta x = 2000$ ).

Quantitative error ratings	Global error (m <sup>3</sup> )	Local error (m <sup>3</sup> )	Constituent error (m)
*****	$E < 0.0070$	$E < 0.0010$	$E < 0.0011$
****	$0.0070 \leq E < 0.015$	$0.0010 \leq E < 0.0050$	$0.0011 \leq E < 0.0050$
***	$0.015 \leq E < 0.050$	$0.0050 \leq E < 0.010$	$0.0050 \leq E < 0.010$
**	$0.050 \leq E < 0.10$	$0.010 \leq E < 0.10$	$0.010 \leq E < 0.050$
*	$E \geq 0.10$	$E \geq 0.010$	$E \geq 0.050$

that if Green's theorem is applied to the finite amplitude term  $g\nabla\zeta$  in the momentum equation, then this boundary term must be interpreted as external to the domain in order to realize stable, accurate, mass conservative results. Alternative interpretations (for example, treating specified flux as both essential in the momentum balance and natural in the continuity equation) that were tested led to unstable algorithms.

CONVERGENCE STUDIES

When  $C^0$  polynomials are used as the approximating function in (7), a discontinuity may exist between the external flux computed from the boundary integral and the flux computed using nodal velocity times the fluid depth (the nodal flux). As discussed earlier, this discontinuity can be viewed as a measure of the approximation error in the discrete equations. For a consistent algorithm the error should approach zero as the grid is refined. Accordingly, we undertook a convergence study to examine the discontinuity error at the boundaries. Errors were evaluated by comparing the time series response for the external flux with the time series of flux computed from the nodal velocity and nodal water depth. As the grid is refined, the difference between the two time series curves should approach zero. Results shown in Figures 4 and 5 demonstrate that the time series do converge as the grid is refined at both the open boundary and the land boundary.

An alternative way to measure convergence at the boundary is to plot error versus grid spacing on log-log paper. For a convergent scheme the error should approach zero as the grid size goes to zero, and the rate of convergence can be found from the slope of the curve. Figure 6 shows the results of this convergence test for both the open ocean boundary and the land boundary where the error was computed as the average of the absolute difference between external flux and nodal flux, i.e.

$$\text{error} = \frac{\sum_{k=1}^{N_T} |Q_k^{\text{nodal}} - Q_k^{\text{external}}|}{N_T}, \tag{22}$$

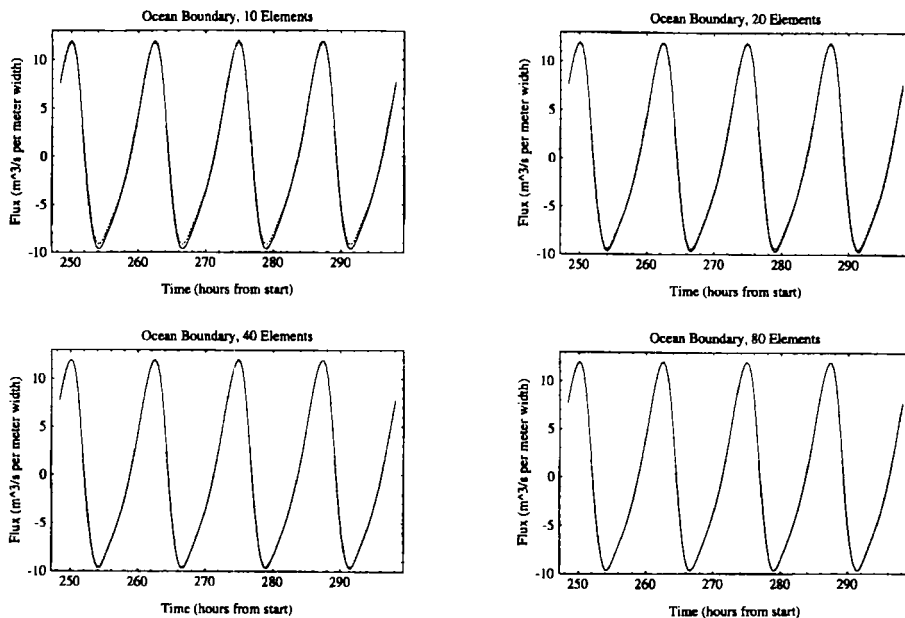


Figure 4. Results of grid convergence studies showing time series response of fluxes at open ocean boundary for various levels of discretization. Full curve is external flux; broken curve is nodal flux

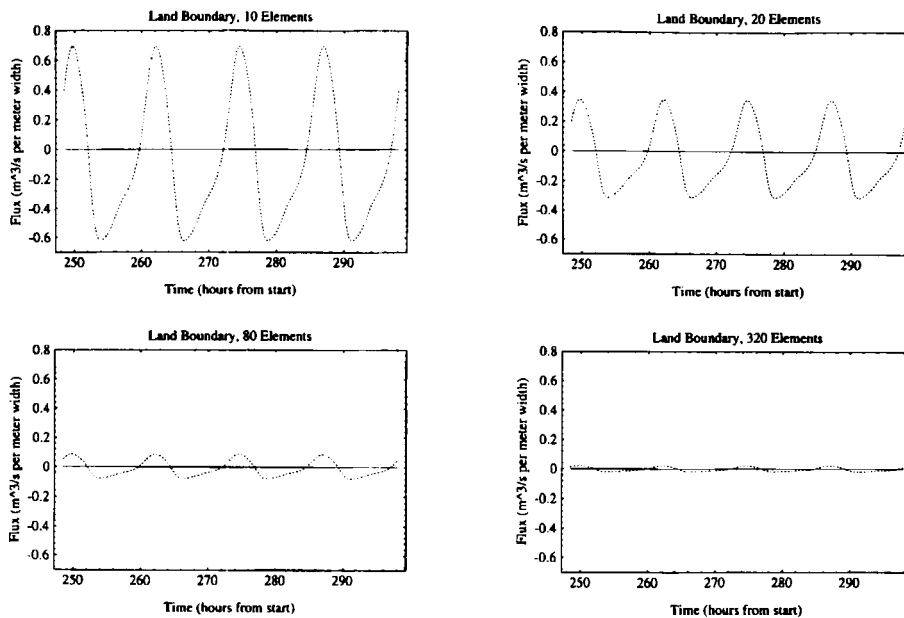


Figure 5. Results of grid convergence studies showing time series response of fluxes at land boundary for various levels of discretization. Full curve is external flux; broken curve is nodal flux

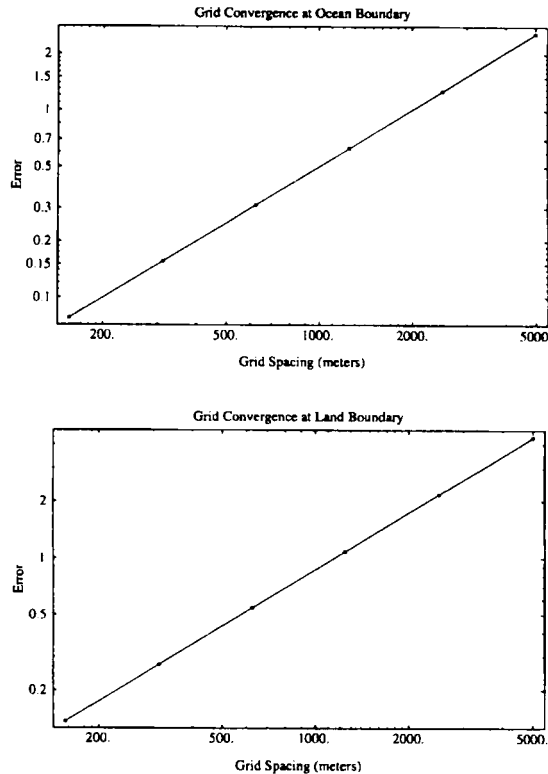


Figure 6. Rate of convergence at both boundaries. Error is average value of difference between nodal flux and external flux (see equation (22))

where  $N_T$  is the number of time steps. As can be seen, the scheme is convergent with a first-order rate of convergence. In contrast, the mass balance errors that arise with some conventional formulations<sup>16</sup> do not diminish as the grid is refined, an indication of an inconsistent algorithm.

## CONCLUSIONS

Shallow water models based on a finite element solution of the wave continuity equation have evolved as powerful tools for simulating the hydrodynamic behaviour of coastal and oceanic waters. However, in some applications, particularly when the non-linear terms are significant, the algorithm may be susceptible to mass balance errors and errors in the generation of non-linear constituents. Herein it is proposed that one source of the error is the treatment of boundary conditions. In particular, a unique derivation using generalized functions shows that the state variable in boundary integrals (that results from application of Green's theorem to the weighted residual form of the governing equations) should be interpreted as external to the computational domain. This interpretation can be viewed as the finite element counterpart of imaginary nodes (nodes outside the boundary) used in finite difference algorithms. Numerical experiments demonstrate that this interpretation does improve the accuracy and consistency of the simulator.

## ACKNOWLEDGEMENT

This research was supported in part by the National Science Foundation under project number DMS-9408151.

## APPENDIX: NOMENCLATURE

<b>A</b>	stress at water surface ( $L^2/T^2$ )
<b>G</b>	numerical parameter in generalized wave continuity equation ( $1/T$ )
<b>H</b>	total fluid depth, $h + \zeta$ ( $L$ )
<b>L</b>	length
<b>L</b>	symbol for primitive continuity equation
<b>M</b>	mass
<b>M</b>	symbol for primitive momentum equation, non-conservative form
<b>M<sup>c</sup></b>	symbol for primitive momentum equation, conservative form
<b>Q</b>	volumetric flux, equal to $Hv$ for shallow water flows ( $L^2/T$ )
<b>T</b>	time
<b>T</b>	macroscopic stress tensor ( $M/LT^2$ )
<b>V</b>	volume ( $L^3$ )
<b>W<sup>G</sup></b>	symbol for generalized wave continuity equation
<b>e</b>	element in finite element mesh
<b>f</b>	Coriolis parameter
<b>g</b>	$ g $ ( $L/T^2$ )
<b>g</b>	gravity vector ( $L/T^2$ )
<b>h</b>	bathymetry ( $L$ )
<b>i</b>	spatial index
<b>k</b>	temporal index
<b>n</b>	unit outward normal vector
<b>t</b>	time
<b>u</b>	scalar fluid velocity, $x$ -component if 2D or 3D problem ( $L/T$ )
<b>v</b>	depth-averaged velocity of fluid ( $L/T$ )

*Greek Letters*

$\Omega$	spatial domain ( $\mathbb{R}^n$ for $n = 1, 2$ )
$\varepsilon$	eddy viscosity ( $L^2/T$ )
$\zeta$	elevation of water surface above datum ( $L$ )
$\lambda$	wavelength ( $L$ )
$\rho$	density ( $M/V$ )
$\tau$	bottom friction ( $1/T$ )
$\varphi$	basis function in finite element formulations

*Special Symbols and Operators*

$\nabla$	nabla (grad) operator ( $1/L$ )
$\nabla \cdot$	divergence operator ( $1/L$ )
$\partial\Omega$	boundary of $\Omega$

## REFERENCES

1. C. Taylor and J. M. Davis, 'Tidal and long-wave propagation: a finite element approach', *Comput. Fluids*, **3**, 125–148 (1975).
2. D. R. Lynch and W. G. Gray, 'A wave equation model for finite element tidal computations', *Comput. Fluids*, **7**, 207–228 (1979).
3. W. G. Gray, 'Some inadequacies of finite elements models as simulators of two-dimensional circulation', *Adv. Water Resources*, **5**, 171–177 (1982).
4. I. P. E. Kinnmark, *The Shallow Water Equations: Formulation, Analysis, and Application*, LNE Vol. 15, Springer, Berlin, 1986.
5. R. L. Kolar and W. G. Gray, 'Shallow water modeling in small water bodies', in G. Gambolati *et al.* (eds), *Computational Methods in Surface Hydrology*, Computational Mechanics/Springer, Southampton/Berlin, 1990, pp. 149–155.
6. D. R. Lynch, F. E. Werner, A. Cantos-Figuerola and G. Parrilla, 'Finite element modeling of reduced-gravity flow in the Alboran Sea: sensitivity studies', *Proc. Workshop on the Gibraltar Experiment*, Madrid, 1988.
7. R. A. Luettich Jr., J. J. Westerink and N. W. Scheffner, *ADCIRC: An Advanced Three-Dimensional Circulation Model for Shelves, Coasts, and Estuaries. Report 1: Theory and Methodology of ADCIRC-2DDI and ADCIRC-3DL*, Department of the Army, U.S. Army Corps of Engineers, Washington, DC, 1991.
8. C. E. Naimie and D. R. Lynch, 'Applications of nonlinear three-dimensional shallow water equations to a coastal ocean', *Computational Methods in Water Resources IX*, Vol. 2, *Mathematical Modeling in Water Resources*, in Russel *et al.* (eds), Computational Mechanics/Elsevier, Southampton/London, 1992, pp. 589–608.
9. R. A. Luettich and J. J. Westerink, 'A solution for the vertical variation of stress, rather than velocity, in a three-dimensional circulation model', *Int. j. numer. methods fluids*, **12**, 911–928 (1991).
10. R. A. Luettich, S. Hu and J. J. Westerink, 'Development of the direct stress solution technique for three dimensional hydrodynamic models using finite elements', *Int. j. numer. methods fluids*, **19**, 295–319 (1994).
11. M. G. G. Foreman, 'A comparison of tidal models for the southwest coast of Vancouver Island', in Celia *et al.*, (eds), *Computational Methods in Water Resources*, Vol. 1, *Modeling of Surface and Subsurface Flows*, DWS Vol. 35, Computational Mechanics/Elsevier, Southampton/Amsterdam, 1988, pp. 231–236.
12. J. J. Westerink, R. A. Luettich, A. M. Baptista, N. W. Scheffner and P. Farrar, 'Tide and storm surge predictions using a finite element model', *J. Hydraul. Eng.*, **118**, 1373–1390 (1992).
13. W. G. Gray, 'A finite element study of tidal flow data for the North Sea and English Channel', *Adv. Water Resources*, **12**, 143–154 (1989).
14. C. A. Blain, J. J. Westerink and R. A. Luettich, 'The influence of domain size on the response characteristics of a hurricane storm surge model', *J. Geophys. Res.*, **99**, 18,467–18,479 (1994).
15. J. J. Westerink, R. A. Luettich and J. C. Muccino, 'Modeling tides in the western North Atlantic using unstructured graded grids', *Tellus*, **46A**, 178–199 (1994).
16. R. L. Kolar, J. J. Westerink, M. E. Cantekin and C. A. Blain, 'Aspects of nonlinear simulations using shallow water models based on the wave continuity equation', *Comput. Fluids*, **23**, 523–538 (1994).
17. R. L. Kolar, W. G. Gray and J. J. Westerink, 'Normal flow boundary conditions in shallow water models—influence on mass conservation and accuracy', in Peters *et al.* (eds), *Computational Methods in Water Resources X*, Vol. 2, Kluwer, Dordrecht, 1994, pp. 1081–1088.
18. W. G. Gray and I. P. E. Kinnmark, 'QUIET: a reduced noise finite element model for tidal circulation', *Adv. Eng. Softw.*, **5**, 130–136 (1983).
19. R. A. Walters and R. T. Cheng, 'Accuracy of an estuarine hydrodynamic model using smooth elements', *Water Resources Res.*, **16**, 187–195 (1980).
20. J. Drolet and W. G. Gray, 'On the well posedness of some wave formulations of the shallow water equations', *Adv. Water Resources*, **11**, 84–91 (1988).
21. M. G. G. Foreman, 'An accuracy analysis of boundary conditions for the forced shallow water equations', *J. Comput. Phys.*, **64**, 334–367 (1986).
22. M. Kawahara, 'On finite element methods in shallow water long wave flow analysis', in J. T. Oden (ed.), *Computational Methods in Nonlinear Mechanics*, North-Holland, Amsterdam, 1980, pp. 261–287.
23. G. K. Verboom and A. Slob, 'Weakly-reflective boundary conditions for two dimensional shallow water flow problems', *Adv. Water Resources*, **7**, 192–197 (1984).
24. D. R. Lynch, 'Mass balance in shallow water simulations', *Commun. Appl. Numer. Methods*, **1**, 153–159 (1985).
25. W. G. Gray, *Progress Report: Estuary Modeling by the Finite Element Method*, USGS, Water Resources Division, Reston, VA, 1977.
26. S. Sigurdsson, S. P. Kjaran and G. G. Tomasson, 'A simple staggered finite element scheme for simulation of shallow water free surface flows', in Celia *et al.* (eds), *Computational Methods in Water Resources*, Vol. 1, *Modeling Surface and Subsurface Flows*, Computational Mechanics/Elsevier, Southampton/Amsterdam, 1988, 329–335.
27. S. Sigurdsson, 'Alternative approaches to the wave equation in shallow water flow modelling', in Peters *et al.* (eds), *Computational Methods in Water Resources X*, Vol. 2, Kluwer, Dordrecht, 1994, pp. 1113–1120.
28. J. J. Westerink, R. A. Luettich Jr., J. K. Wu and R. L. Kolar, 'The influence of normal flow boundary conditions on spurious modes in finite element solutions to the shallow water equations', *Int. j. numer. methods fluids*, **18**, 1021–1060 (1994).
29. J. C. Galland, N. Goutal and J. M. Hervouet, 'TELEMAC: a new numerical model for solving shallow water equations', *Adv. Water Resources*, **14**, 138–148 (1991).

30. W. G. Gray and M. A. Celia, 'On the use of generalized functions in engineering analysis', *Int. J. Appl. Eng. Educ.*, **6**, 89–96 (1990).
31. W. G. Gray, A. Leijnse, R. L. Kolar and C. A. Blain, *Mathematical Tools for Changing Spatial Scales in the Analysis of Physical Systems*, CRC Press, Boca Raton, FL, 1993.
32. P. M. Gresho and R. L. Lee, 'Don't suppress the wiggles—they're telling you something', *Comput. Fluids*, **9**, 223–253 (1981).
33. W. Horn, 'The harmonic analysis, according to the least squares rule, of tide observations upon which an unknown drift is superposed', *3rd Int. Symp. on Earth Tides*, Trieste, 1959.
34. A. C. M. van Ette and H. J. Schoemaker, 'Harmonic analysis of tides—essential features and disturbing influences', *Proc. Symp. on Tides*, Monaco, 1967.